JOURNAL OF ENGINEERING RESEARCH AND APPLIED SCIENCES (JERAS)
6th Edition –Volume (1) - December 2018, (Hoon – Libya), **ISSN 2414-6515**

VISUAL DETERMINATION OF CAVITATION DEGREES IN HIGH ENERGY CENTRIFUGAL PUMPS

Ahmed A. B. Alarabi and khaled A. Hassan

a.alarabi@ceh.edu.ly kaled505aa@yahoo.com
Department of mechanical Engineering, College of Engineering Technology – Hoon, Libya

Abstract

In the present paper an experimental investigation using high speed digital camera was carried out in order to find out the cavitation degrees in high energy centrifugal pumps. The used centrifugal pumps were of 10 hp, 20 hp and 30 hp. A special water tunnel was designed and constructed in order to obtain adequate information about incipient, developed and breakdown cavitation in a closed flow system, and hence using it as criteria of cavitation degrees. The experiments were carried in fluid mechanics laboratory at College of Engineering Technology Hoon, Libya.. A special test section of 20mm × 40mm dimension with transparent perspex face was conducted in order represent the represent the point corresponding to 3% drop in head. The photography results showed that the cavity length increases with increasing the flow rate ratio. Using a 30 hp centrifugal pump, a snow-white color cavities were appeared, while a misty white color appears when using 10 and 20 hp centrifugal pumps. Also it was obtained that at B. E. P. the cavity length was varied between 40 mm and 50 mm, while the B.E.P. range was found to be varied between cavity lengths 25 mm to 60 mm. For cavitation performance experiments it was obtained that that incipient cavitation for the test pumps varied between cavity lengths 58 mm to 63 mm. The developed cavitation was obtained at cavity lengths varied between cavity lengths 64 mm to 73 mm. The breakdown cavitation was obtained at cavity lengths varied between cavity lengths 67 mm to 84 mm.

Key worlds: Cavitation, centrifugal pumps, cavity length, cavitation inception, developed cavitation, breakdown cavitation.

1. Introduction

It is well known that the principal effects of cavitation in hydrodynamic systems are erosion to all materials, loss of performance, change in flow pattern, vibration and noise. Due to impossibility to find the incipient of cavitation in hydrodynamic systems theoretically several experimental studies have been carried in order to provide adequate information about incipient and breakdown cavitation in a closed flow system. Moreover, the designer often lacks specific information on how design changes will affect cavitation behaviour of the machine or the system [1]. Changing flow velocity, power loading and size of machines may cause an unexpected cavitation problems. Therefore, the constructed model test becomes very important to predict the cavitation behaviour in prototype and then supplied the designers with useful information which led to a better design.

McNulty PJ, and Pearsall IS, (1982) carried a research concentrated on cavitation inception in centrifugal pumps. The study was focused on the criteria of cavitation occurrence and its relation with the pump head and pump efficiency. He concluded that the inception of cavitation occurred when the pump head dropped by 1 to 10 percent. This means that less than this

percent the pump performance not affected (i.e. no cavitation occurred).

D. P. Hart et al. (1990), have designed and constructed an experimental test rig to observe the effect of sinusoidal pitching oscillations on the cavitation of three-dimensional hydrofoils. The apparatus is capable of oscillating hydrofoils at a rate up to 50 Hz and. Several photographs have been taken at different frequency degrees in order to observe the leading edge cavitation, and cavitation was observed from inception degree at the suction side of the hydrofoil, till developed cavitation degree at the trailing edge. The variation of the cavitation number with hydrofoil phase angle and geometric angle of attack were obtained at different excitation frequencies.

A. Konno, et. Al.,(1999), have observed the collapse of cavitation bubble clusters on a two-dimensional foil. The high-speed video was taken at a speed of 40,500 fps. Duration of collapse was the order of 10 to 100 microseconds, which was by far slower than that of an impulsive force that was around 5 microseconds. They reported that by calculations the impulsive pressure is generated when the cloud cavity collapses completely. But they found experimentally, that the peaks of impulsive force did not meet the instant of final collapsing, but were often some 10 to some 100 microseconds earlier than the final collapsing. The results suggest that an impulsive force may not be caused by the global behaviour of a bubble cluster but by the behaviour of a part of cloud cavity. The collapse of a large single bubble in the cloud cavity and generation of micro-jet may cause such phenomenon. They agreed that this new finding should be verified more experimentally as well as theoretically.

Sheng-Hsueh Yang et al.(2009), have carried an experimental investigation to study the bubble collapse visually They used a device of U-shape platform to generate a single cavitation bubble for a detailed analysis of the flow field characteristics. The bubble was collapsed by sending a pressure wave. They used a high speed camera to record the flow field of the bubble collapse at different distances from the solid boundary. The strength of the pressure wave was adopted to induce the bubble collapse flow is kept as low as possible so that the bubble collapses in a longer period of time. They found that a Kelvin–Helmholtz vortex is formed when a liquid jet penetrates the bubble surface after the bubble is compressed and deformed.

Alarabi and Selim (2009), carried an experimental work for studying the cavitation inception in centrifugal pumps. The study based on the visual observation where a special Perspex face of suction side was manufactured for visual process. Several photographs at different operating conditions have been taken. According to the experimental results an empirical relationship between the visual NPSH and NPSH corresponding to 3% drop in head, taken into account three different parameters flow rate ratio, pump rotational speed and water temperature, it was obtained that the inception of cavitation occurred much earlier than that value corresponded to 3% drop in the head.

Tzanakis, I. and Hadfield, M., (2010), carried an experimental study using an ultrasonic transducer, submerged into the fluids (water-lubricant-refrigerant), to produce cavitation bubbles. Different images were focused on two critical areas: the lower surface of the horn and across the boundary of the sample. The sample consists of a chromium ball mounted on a Bakelite base and implemented on the bottom of the experimental tank. The results revealed that the lubricant bubbles have a similar behaviour to those produced in water, and the damage produced by the refrigerant bubbles is smaller than that observed within water and oil lubricant., and also the lubrication thickness layer developed across the boundary was observed to provide a cushion, absorbing the jet impact during the implosion of a bubble

A. **A. Alarabi, (2012),** Studied cavitation phenomenon in closed flow system . A special water tunnel was designed and constructed at fluid mechanics laboratory at College of Engineering Technology, (Hoon – Libya), The water tunnel has a test section with dimensions (20 mm × 40 mm) with a transparent face to permit the cavitation observation. Different cavitation sources with circular and triangles shapes have been used in order to create a cavitation in the test section. Alarabi has recorded different visible cavitation degrees. He concluded that the cavity length increases with the increase of flow rate till reaching the break down point, and the inception cavitation number decreases with increase of flow velocity. It is obtained that the cylindrical source body can be used as a cavitation source for a wide range of flow rates for the current flow system.

Bram Verhaagen, et all, (2016) , reviewed several techniques for measuring the presence and amount of cavitation, and for the quantification of cleaning. They reported that after reviewing chemical, physical, and biological studies, a universal cause for the cleaning effects of bubbles cannot yet be concluded. They proposed an ‘‘ideal sensor’’ with high spatial and temporal resolution to investigate bubble jetting, shockwaves, streaming, and even chemical effects, by correlating cleaning processes with cavitation effects, generated by hydrodynamics, lasers or ultrasound.

B.K. Sreedhar et. al. (2017), presented a review study to understand cavitation damage. The study covered the theoretical formulation of cavitation bubble collapse and the estimate of bubble collapse pressure, the techniques for measurement of cavitation damage in the laboratory and the special facilities for measurement of cavitation damage in sodium, the instrumentation for measurement of collapse pressure during cavitation as well as the work done in predicting damage from material properties. The limited success in achieving good damage prediction was discussed. They reported that the major reason for the limited success of cavitation erosion models based on bulk mechanical properties may be due to the inability to account for the behavior of materials under the very high strain rates (104– 106 /s), as occurs under cavitation ,as opposed to the almost static loading conditions under which bulk mechanical properties are measured. Another reason for the limited success in damage prediction may be attributed to the change in the behavior of materials (for e.g. strain hardening) under cavitation loading

Hou-lin Liu et al. (2014), considered a homogenous model, the Zwart-Gerber-Belamri cavitation model, to investigate the influence of the empirical coefficients on predicting the pump cavitation performance, concerning a centrifugal pump. They analyzed three coefficients which are the nucleation site radius, evaporation and condensation coefficients. An experimental work were carried to validate the numerical simulation. The results indicated that, to get a precise prediction, the approaches of declining the initial bubble radius, the condensation coefficient or increasing the evaporation coefficient are all feasible, especially for declining the condensation coefficient, which is the most effective way. Compared with the experiment, the computed results show that the accuracy of the predictions of the pump cavitation performance is improved as the nucleation site radius decreasing. It is concluded that, the evaporation coefficient controls both the cavity length and the high vapor volume fraction cavity region, and the later factor is more affective on the pressure loading on the blade, but less effective on numerical predictions. it is observed that, when the cavity covers all over the suction side of the blade, the simulation result has the best agreement with the experiment. However,

while the cavity length is within the blade, the simulation results have only a little change.

Xiongjun Wu et. Al. (2017), had built a 2D convergent-divergent test section to study sheet cavitation followed by bubble cloud formation experimentally, where flow visualizations and pressure measurements enabled correlating high speed photography observations with the pressures on the cavitating surface. They indicated that the frequency of the recurring sheet cavity decreases with increased inlet flow velocity. It is indicated also that with increase of inlet velocity, the flow structure changes from vortex shedding with entrapped thin cavities, to a sheet cavity with a reentrant jet producing bubble cloud shedding, to a shock dominant cavity collapse flow regime.

They concluded that when the shock forms, the shock front moves much faster toward upstream than the reentrant jet does, and the measured shock velocities are an order of magnitude higher than the reentrant jet velocities and exceed the local sound speed.

A. A. Alarabi and k. A. Hassan (2017), presented an experimental investigation concerning visual determination of best efficiency point in high energy centrifugal pumps using high speed camera**.** The best efficiency point was represented by the cavity length in the test section. They concluded that at B. E. P. the cavity length was varied between 40 mm and 50 mm, while the B.E.P. range was found to be varied between cavity lengths 25 mm to 60 mm.

2. GENERAL RIG DESCRIPTION

All parts of the test rig were designed, to withstand the working stress levels. The pump was specified to overcome the head losses in the rig. The liquid leakage out of the pump can be controlled by using rubber packing, which was compressed to give the desired fit on the shaft by a gland that can be adjusted in an axial direction. The packing prevents the air leakage into the pump at any working condition where the interior of the stuffing box end is below atmospheric. The test rig dimensions were evaluated from the considerations of economy and hydrodynamic efficiency .

The general arrangement of the test rig is indicated in a schematic diagram shown in figure 1. The flow system consists of the tested centrifugal pump with , the main tank, the test section, the suction, delivery and by-pass lines. The orifice, measuring devices (orifice meter, pressure gauges, and U-manometer) , and valves . By-pass delivery pipe is used for accurate adjustment of the flow in the test section specially in the of using high power pumps.

The pump is positioned on a special concrete stand where the water level in the tank is (120 cm) higher the level of suction pipe centerline. The pump is connected with suction, and delivery pipes of 2 inch. Four gate valves, one is located at distance of 30 cm from the pump entrance, and two valves located in main delivery pipe one of them before the test section by 50 cm and the other after the test section by 50 cm, the fourth gate valve is located in the by-pass pipe for precise adjustment. These valves are used to establish the performance and cavitation test of the pump.

With a general-purpose cavitation tunnel it is highly desirable to have means of adjusting and controlling the test section flow velocity, since many of fundamental parameters of fluid flow are functions of this variable. To achieve this requirement, a test section water tunnel is incorated with the pump circuit as shown in figure 1. The working section is a rectangular cross section of 40x20 mm. The upper face of the test section was built with a transparent prespex with dimension 260×40mm to permit visual study. The tunnel has the capability of operating at various flow velocities over a wide pressure ranges. The flow velocity and pressure can be regulated till a maximum value of 40 m/s and 8 bar respectively by means of a bypass line control. A U-tube manometer was used to measure the volume flow rate. The upstream

static pressure was measured using Bourdon pressure gauge (0-7 bar) connected at three points of the test section in order to obtain an accurate value by taking the average of the three average values. Three centrifugal pump of electric power 10 hp, 20 hp and 30 hp were used to satisfy the requirements of operating system. The suction line, delivery line and by pass line were of diameters 3", 2" and 2" respectively. The main tank has a volume of 0.191 m^3 and it is made of cylindrical shape in order to avoid the turbulence phenomenon. When the tunnel operated at the first time, the water temperature increased rapidly due to the friction between the water and the inside walls of the pipes. To maintain a constant water temperature a special cooling unit was connected with main tank to keep the water temperature at a range (28 ^oC – 30 ^oC). Equation (1) shows the variation of water temperature with the time

$$T = 0.672\ t - 0.007276\ t0.8 \quad (1)$$

Where: T- The water temperature (^oC)
t – The time (sec)

1. The main tank	6. The discharge line	11. By pass line
2. The suction line	7 & 13. The control valve	12. The control unit
3. The centrifugal pump	8. The test section	14. Refrigeration unit
4. The electric motor	9. The orifice	15. The refrigeration unit pump
5. The pump base	10. The U- manometer	

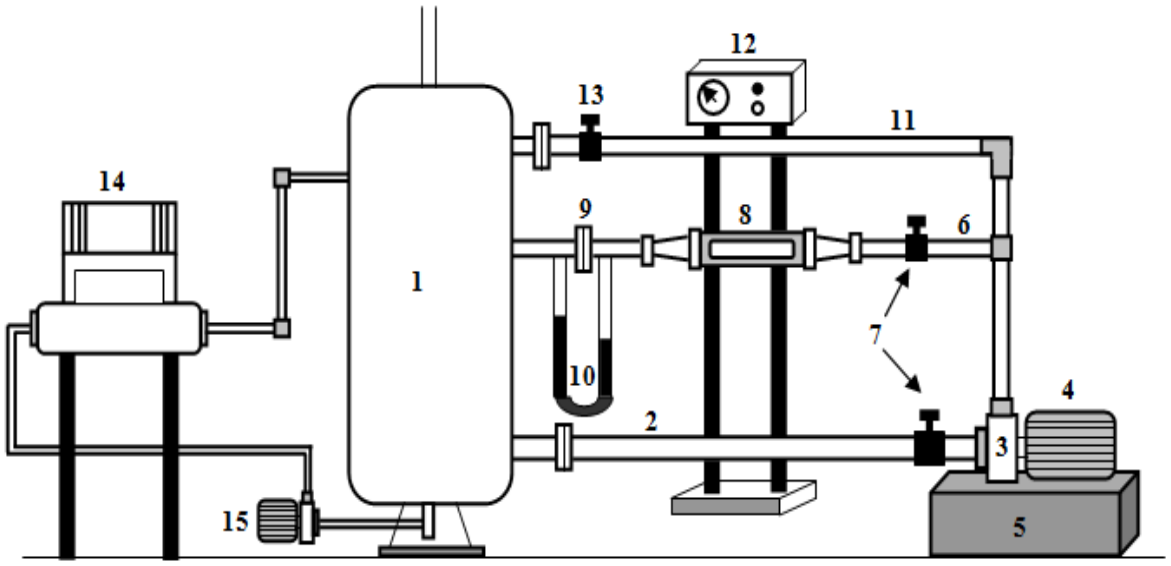

Fig. 1 Test rig construction

3. Results and discussion

Figures 2 - 4 show the effect of NPSH on head with various values of flow rates (Q/Qopt). The flow rate ratio was varied from 0.5 to the maximum flow rate.

Generally theses figures show that the maximum available net positive suction head values is dependent upon the flow rate. The observed trend is that the value of maximum available net positive suction head increases with decreasing the flow rate. The cause of increasing the available net positive suction head with decreasing the flow rate can be attributed to the increase of the flow velocity with flow rate and the decrease of the suction pressure with flow rate. The combination of these two functions should cause an increase of maximum available net positive suction head with decreasing flow rate. Therefore, it is evident that with increasing flow rate the decrease in suction pressure is larger than the increase in velocity head of the flow which is proportional to the square of the velocity.

Figures 2 - 4 indicate, for all operating conditions tested, that the head rise across the pump is maintained nearly a constant value from the maximum available net positive suction head down to the inception condition (NPSHi). As the NPSH is decreased down to near the breakdown of the pump head, the head rise remains nearly unchanged, there is a tendency for the head rise across the pump to decrease as the NPSH decreases for developed cavitation condition. A possible explanation for this trend is that at lower flow rate ratio the circulatory flow at the pump inlet is increased causing an increase in the hydraulic losses and causing a slight decrease in head. In addition at lower flow rate ratios, the liquid enters the impeller at a larger incidence blade angle. This may create a dead space in the region where cavitation usually develops.

For further reduction in the NPSH towards the breakdown condition the energy rises across the pump reduces rapidly and the performance breakdown occurs. This may be attributed to that at lower NPSH the cavitation zone extends rapidly and the size of cavitation zone exceeds that of the dead space. This trend is in agreement with statement of Yedidiah (1980) who stated that as the vapour filled area is not larger than the dead space, performance is not affected. Performance breakdown after the available NPSH is lowered to point where the size of the cavitating zone exceeds that of the dead space

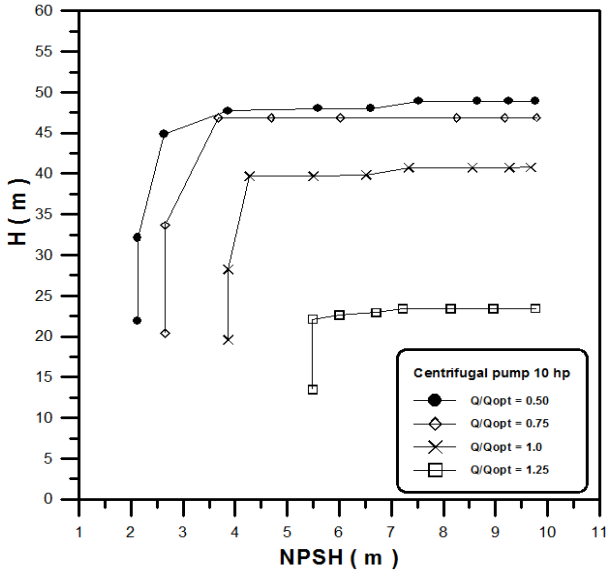

Fig. 2 Variation of NPSH with pump head at different flow rate ratio (10 hp)

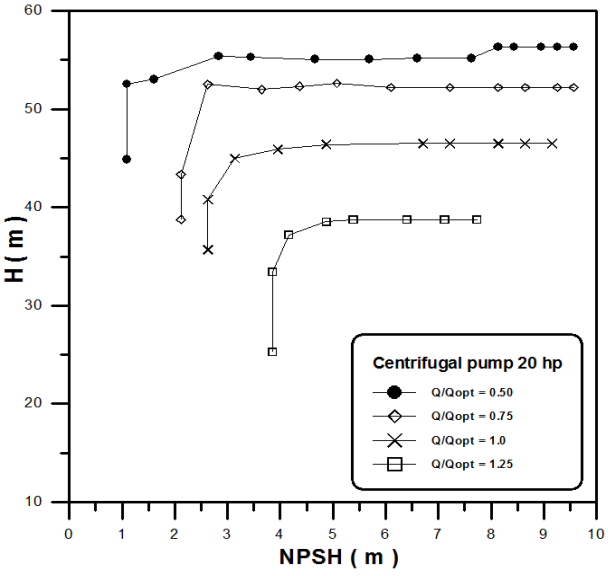

Fig. 3 Variation of NPSH with pump head at different flow rate ratio (20 hp)

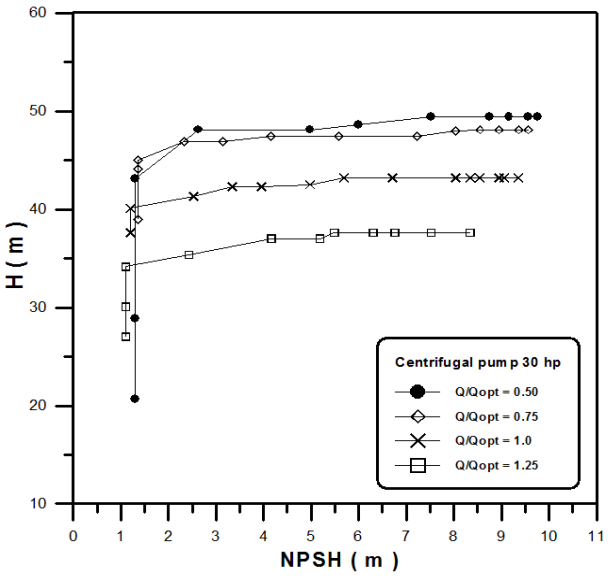

Fig. 4 Variation of NPSH with pump head at different flow rate ratio (30 hp)

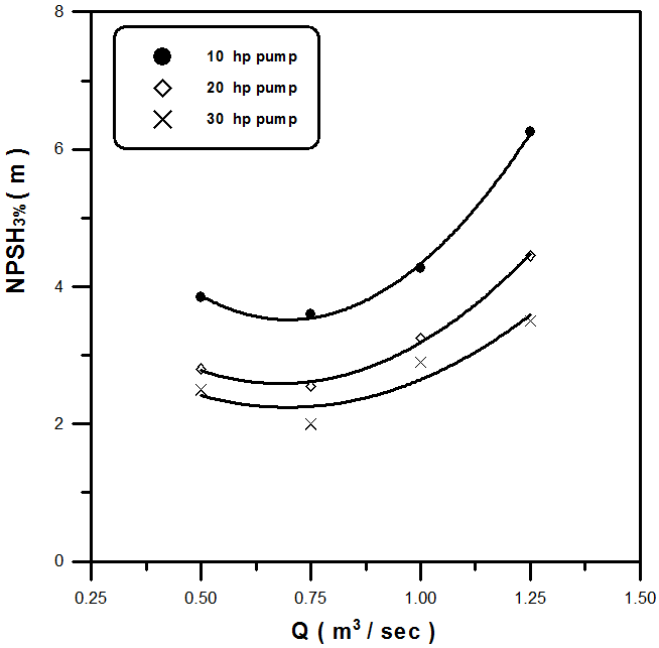

Fig. 5 Variation of NPSHi with flow rate ratio

3.1 VARIATION OF $NPSH_i$ WITH FLOW RATE RATIO

Figure 5 indicates that for all test conditions the NPSHi depends strongly on the flow rate ratio. The flow rate ratios were ranged from 0.5 to 1.25. The general trends of the NPSHi versus flow rate ratio curves are that the NPSHi decreases with increasing the flow rate ratio, reaches a minimum and then increases with increasing the flow rate ratio. Similar trend was reported by Pearsall (1982), Worster, D. M. and Worster, C. (1983), Selim et. al., (1989), Grist (1986)2 and Hofmann, M. et, al (2001). However, the present trend is somewhat contrary to the trend reported by other investigators Gourbiere P. et. al., (1982), Chalaby and King Thew (1982) and Verga et. al., (1969) who reported from their experiments that the critical cavitation number defined by 2% reduction of the head increased with increase in the flow rate. It is believed that in their experiments the range of flow rate may be larger than the optimum flow.

Figures from 6 – 9 presented the photographs of cavitation degrees of 10 hp pump on (H-NPSH) curve. Using 10 hp pump no cavities were appeared in the incipit cavitation rang. This approved the absence of cavitation in the pump. From the figures it can be seen that at high NPSH no cavities were appeared for all flow rates. At developed cavitation the cavities appeared with an average length of 65 mm approximately. Figure 3.66 shows the photography representation of H-NPSH curve at Q/Qopt = 1.25. Increasing the flow ratio to this values enabled us to take the photos at incipit, developed and breakdown cavitation. According to the cavitation occurrence, it can be concluded that the photos are matched well with the H-NPSH curve. Breakdown has the highest degree of cavitation at pump inlet which is then traveled with flow in pipe line through the test section. This means that if any of the degree occurred in the pump section, its degree can be noticed in the test section which is the main objective of the carrying work.

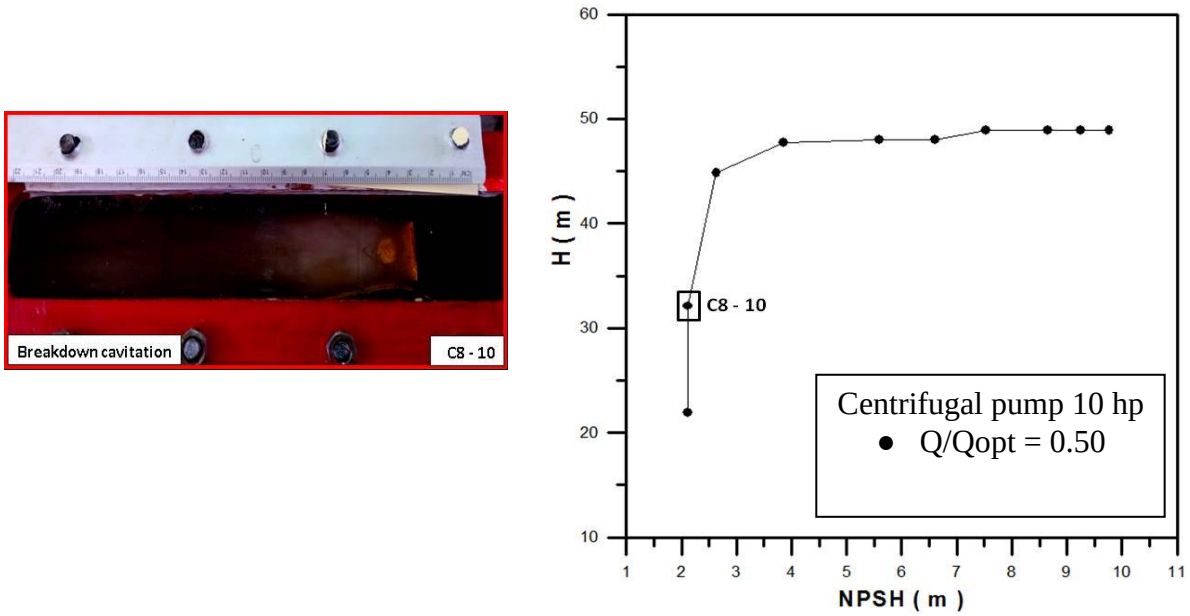

Fig. 6 Photography representation of H-NPSH curve at (Q/Qopt = 0.50) 10 hp pump

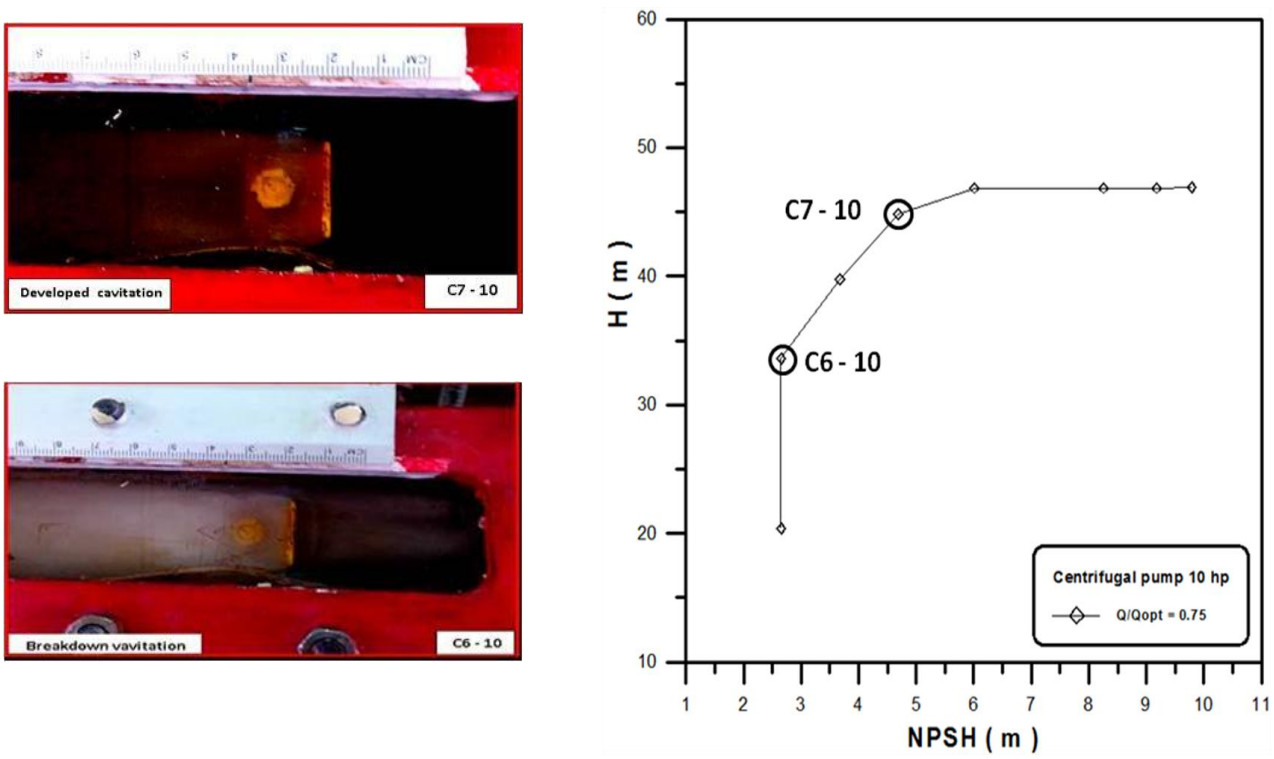

Fig. 7 Photography representation of H-NPSH-curve at (Q/Qopt = 0.75) 10 hp pump

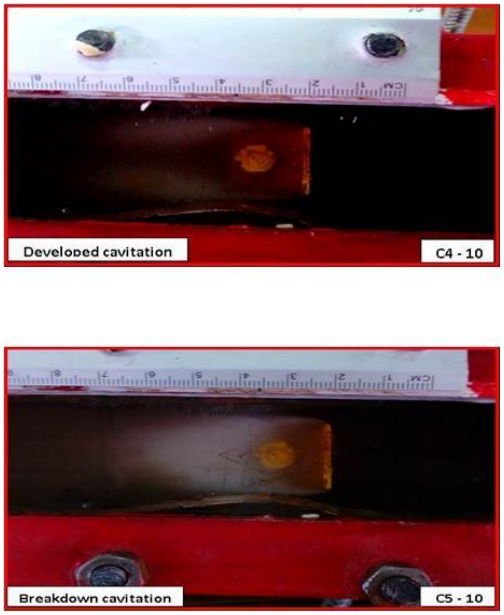

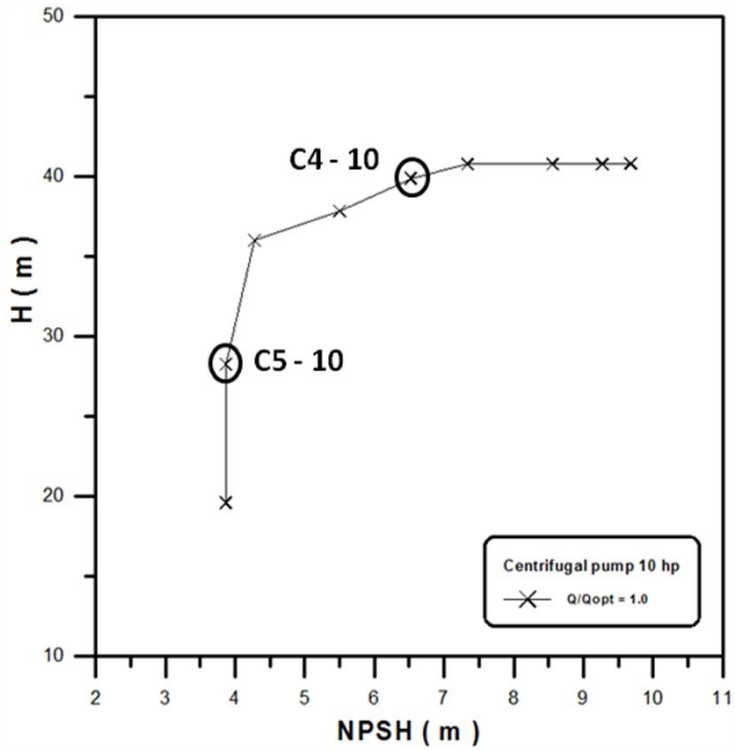

Fig. 8 Photography representation of H-NPSH-curve at (Q/Qopt = 1.0) 10 hp pump

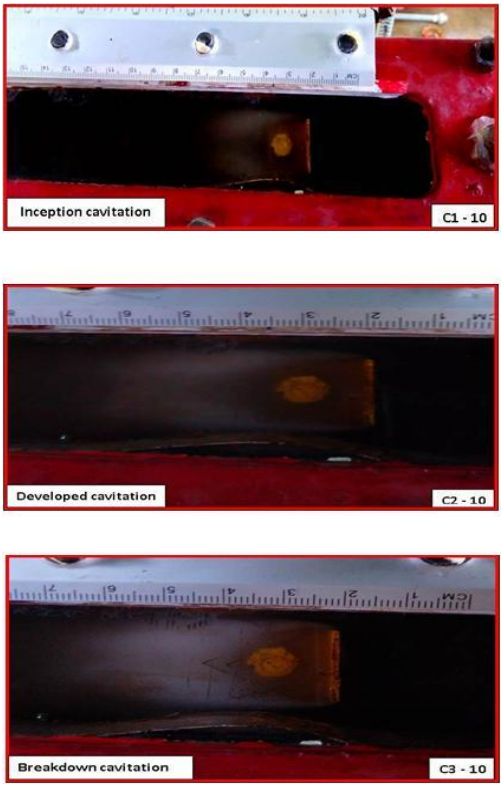

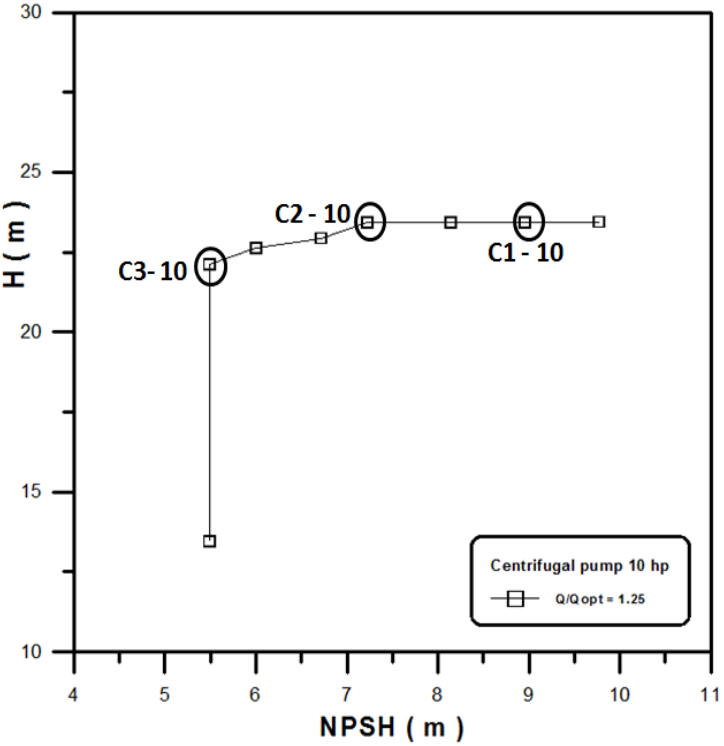

Fig. 9 Photography representation of H-NPSH-curve at (Q/Qopt = 1.25) 10 hp pump

Figures from 10 - 12 presented the photographs of cavitation degrees of 20 hp pump on (H-NPSH) curve. Testing this pump no cavities were achieved in the test section, but this cannot confirm the absence of cavitation in the pump section. It can be noticed that in these figures the cavitation degrees appeared clearly and the cavities color are more white compared with 10 hp results. The cavity length increases with the increase of the cavity degree. According to the recorded cavity lengths it was found that the cavity in incipit, developed and breakdown cavitation 58.33mm, 73mm and 83.33mm respectively. Interface between the cavity lengths sometimes occurred and this is mainly happened due the fluctuating resulted from flow circulation of the flow at the pump section.

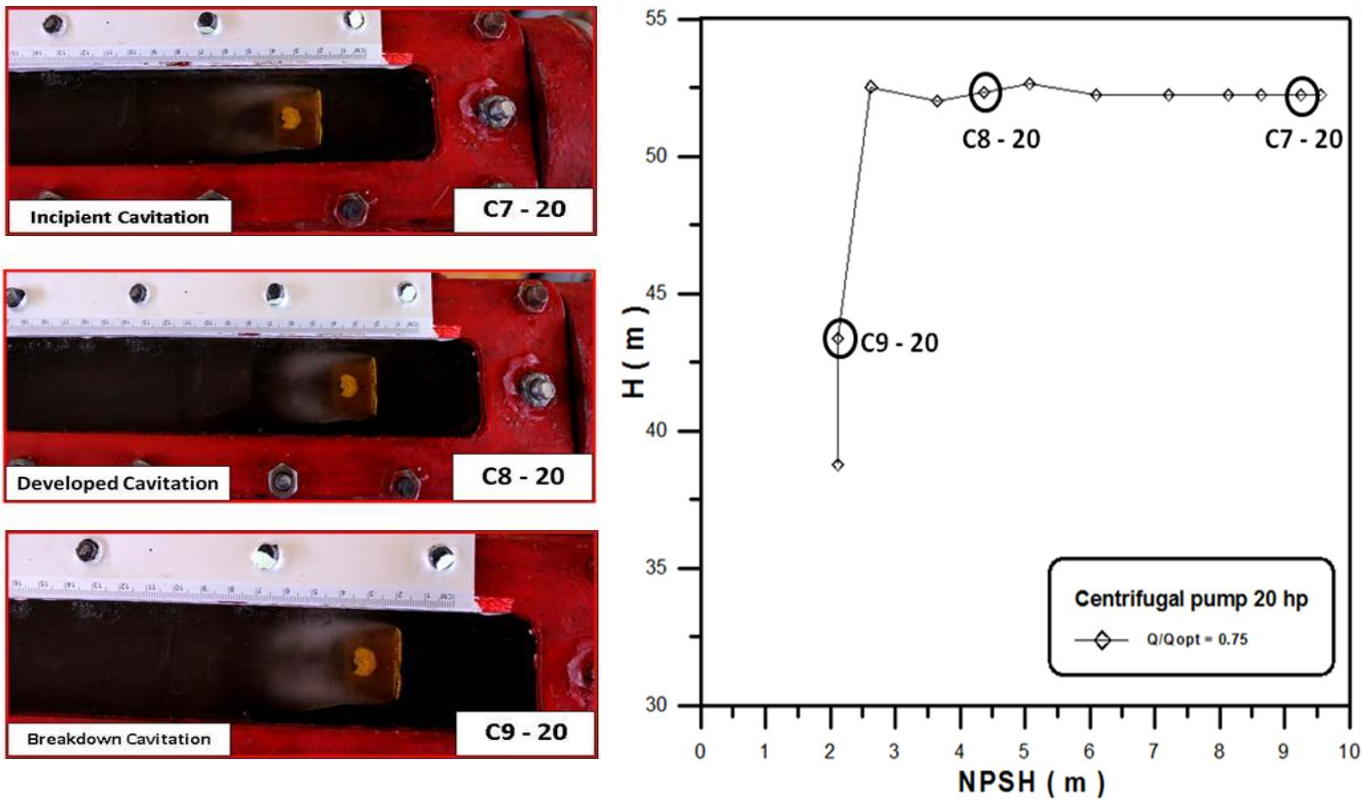

Fig. 10 Photography representation of H-NPSH-curve at (Q/Qopt = 0.75) 20 hp pump

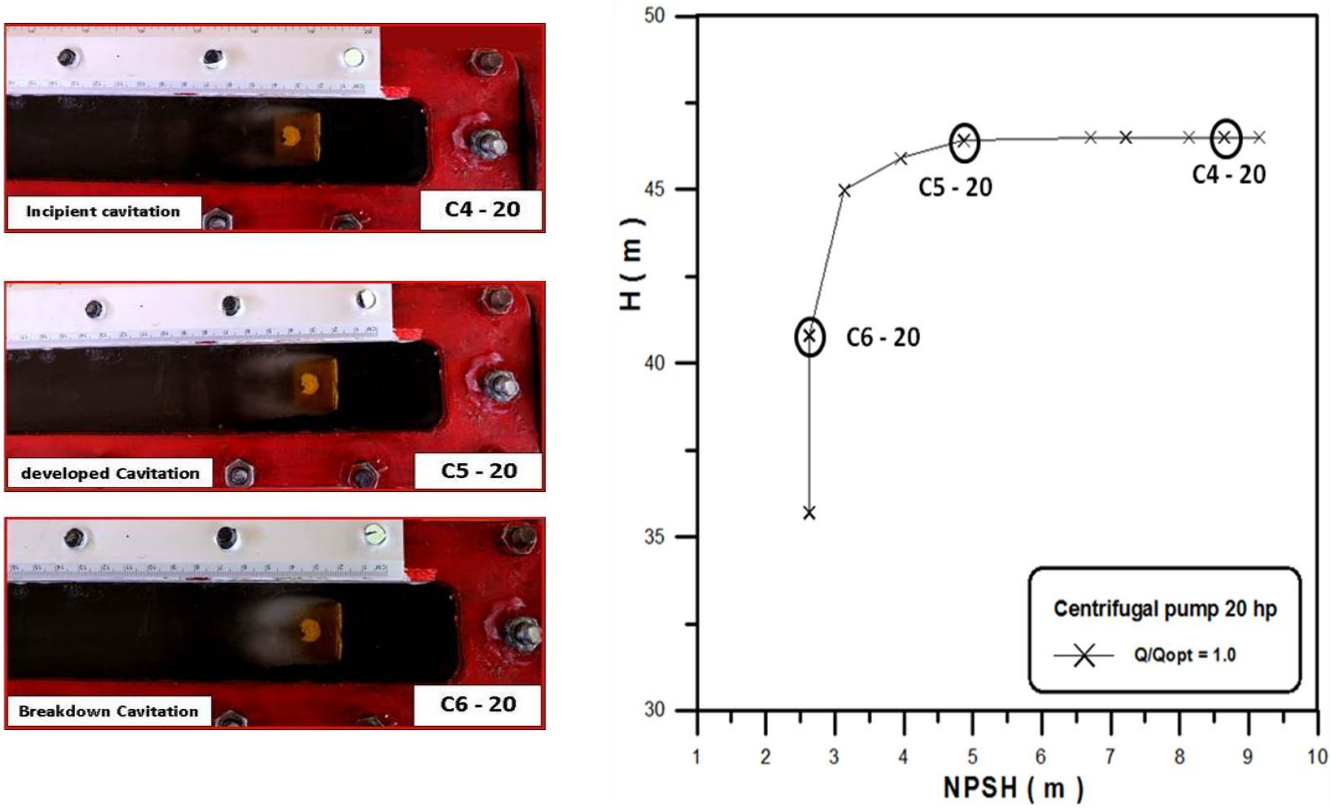

Fig. 11 Photography representation of H-NPSH-curve at (Q/Qopt = 1.0) 20 hp pump

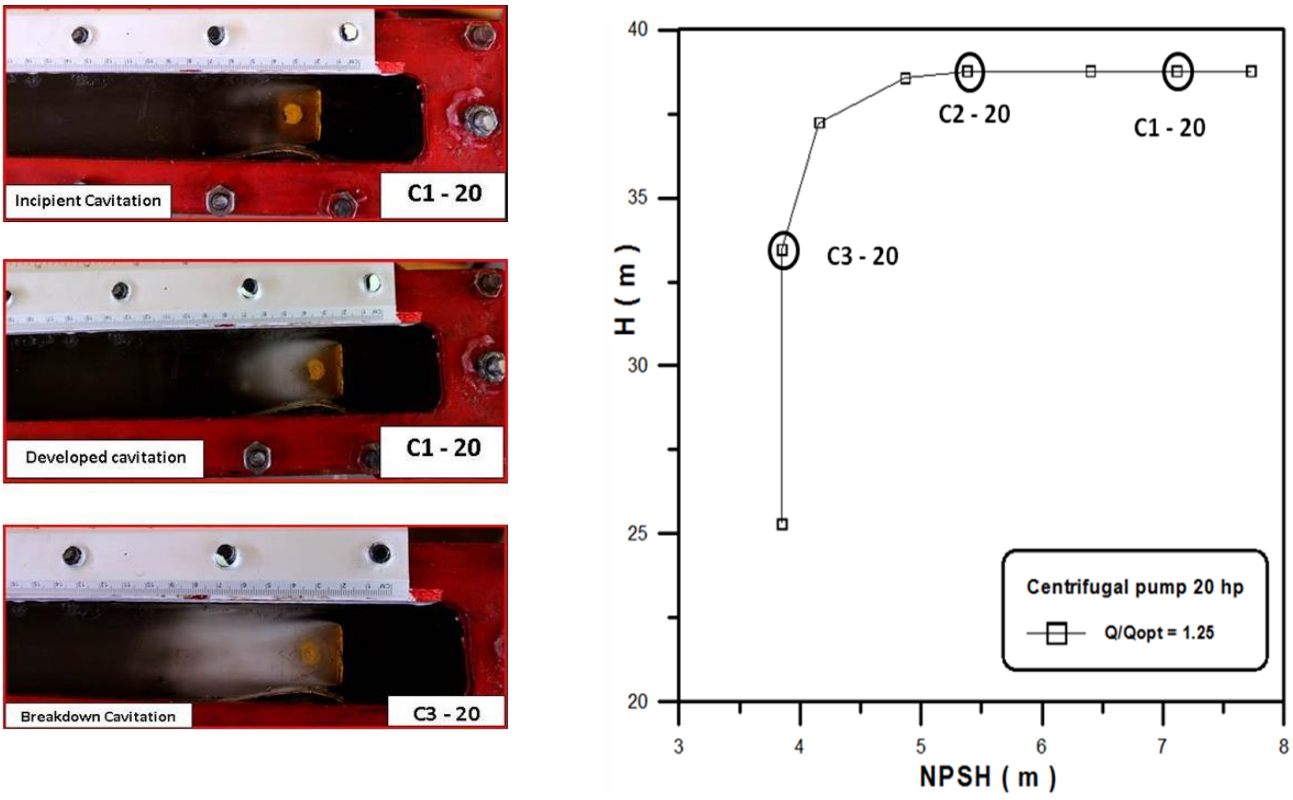

Fig. 12 Photography representation of H-NPSH-curve at (Q/Qopt = 1.25) 20 hp pump

Figures from 13 - 15 presented the photographs of cavitation degrees of 20 hp pump on (H-NPSH) curve. It can be seen that there is a very small difference in cavity between 30 hp pump and 20 hp pump, see table 10. The cavity length in most flow rate ratios was measured except that for flow rate ratio (Q/Qopt = 1.25) at the break down the cavities covered the test section completely, and this mainly occurred due to high flow velocity. The figures show that density of cavities increases with the increase of pump power, so that 30 hp pump has the highest density of cavities. Also the color of cavities in this condition was much pure and achieved the highest whiteness degree.

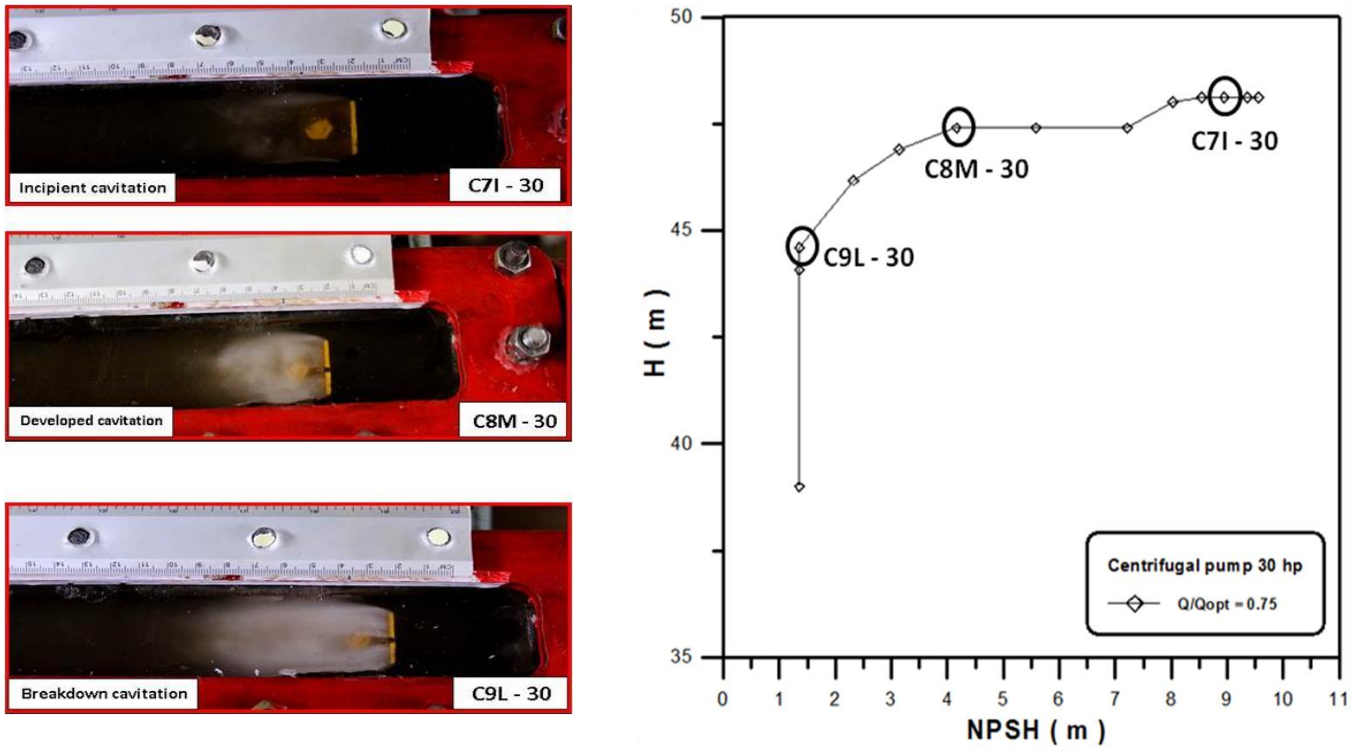

Fig. 13 Photography representation of H-NPSH-curve at (Q/Qopt = 0.75) 30 hp pump

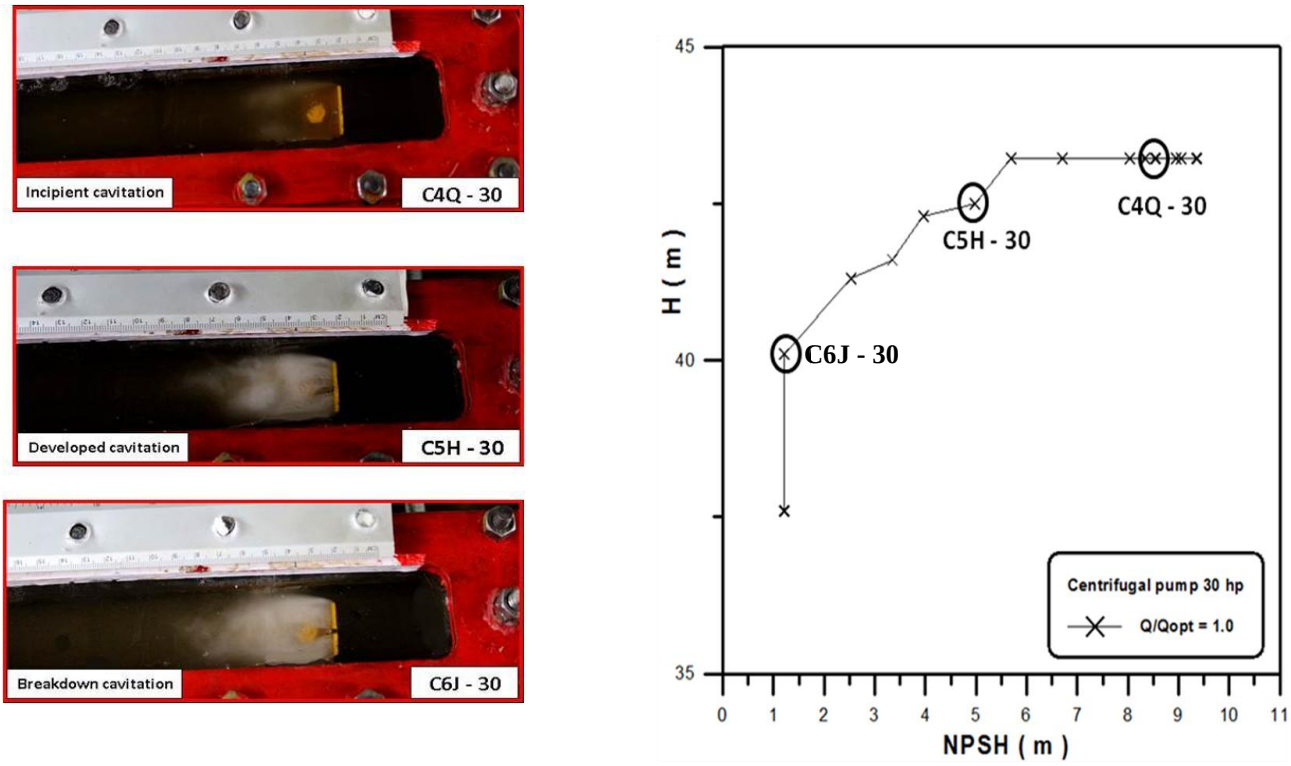

Fig. 14 Photography representation of H-NPSH-curve at (Q/Qopt = 1.0) 30 hp pump

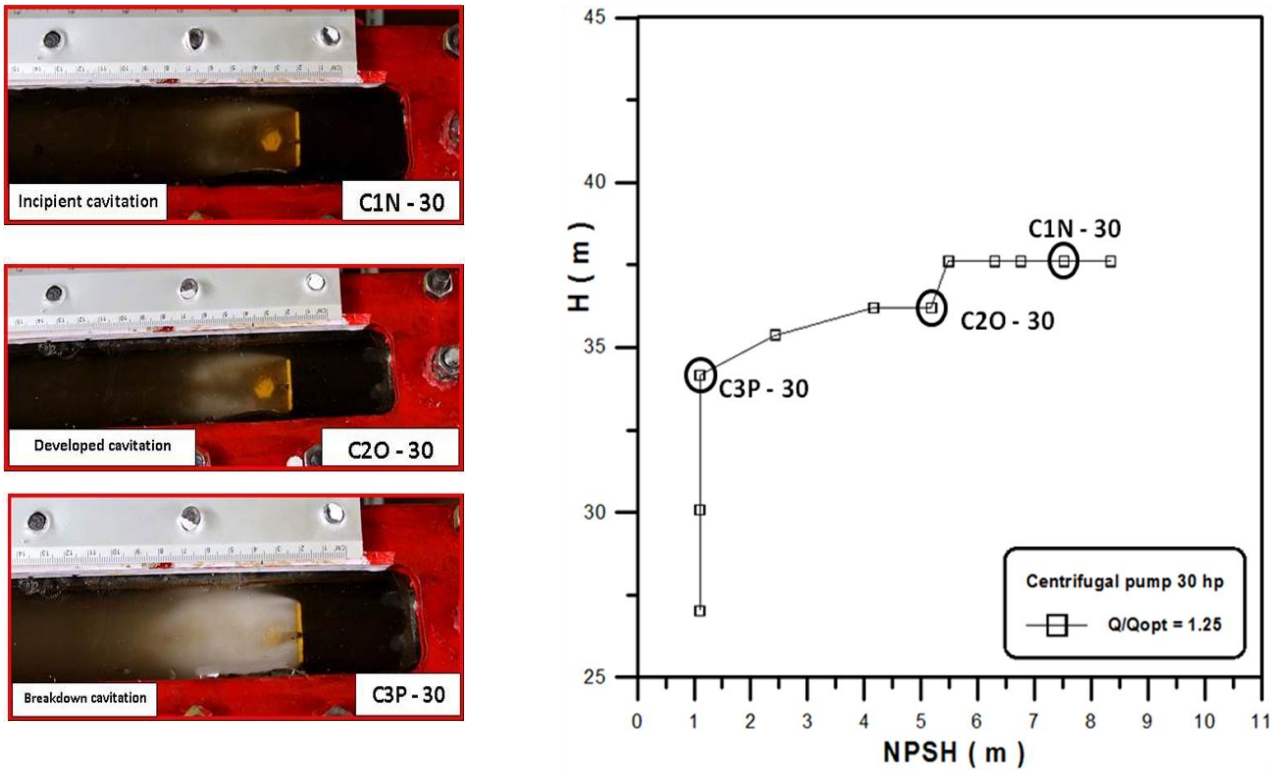

Fig. 15 Photography representation of H-NPSH-curve at (Q/Qopt = 1.25) 30 hp pump

Based on the results obtained in the figures 16, 17 and 18 and on the convergence of the cavity length values, the average of cavity length values for incipit, developed and break down cavitation at the corresponding flow rate ratios of all pumps were calculated and plotted in figure 19. From this figure it can be concluded that to avoid the cavitation in the tested pumps, the cavity length should be less than 60 mm.

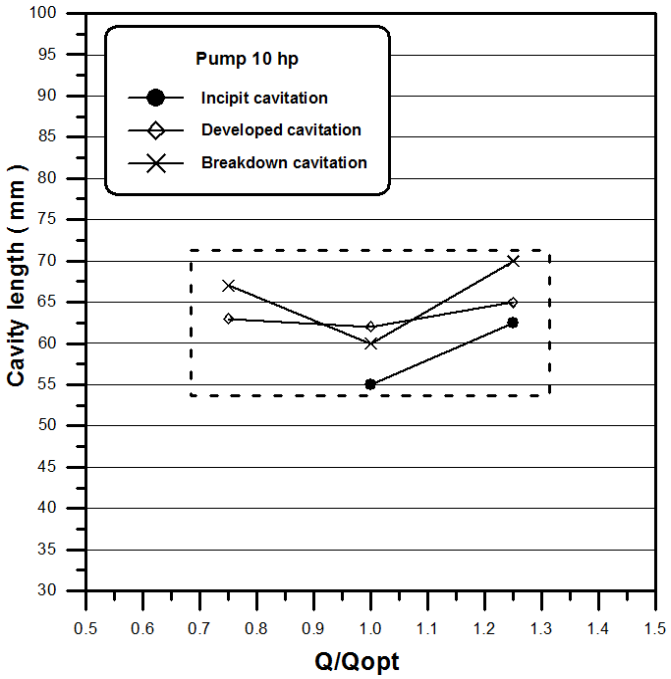

Fig. 16 Variation of cavity length with flow rate ratio for 10 hp centrifugal pump

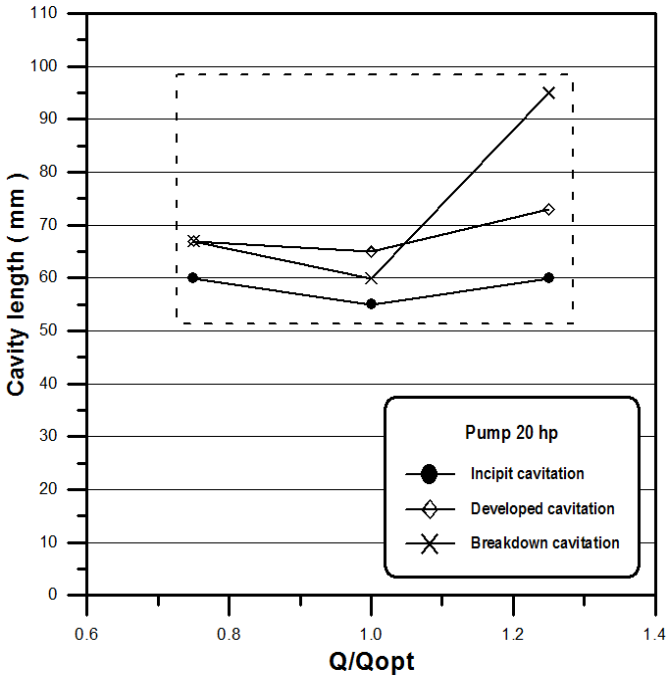

Fig. 17 Variation of cavity length with flow rate ratio for 10 hp centrifugal pump

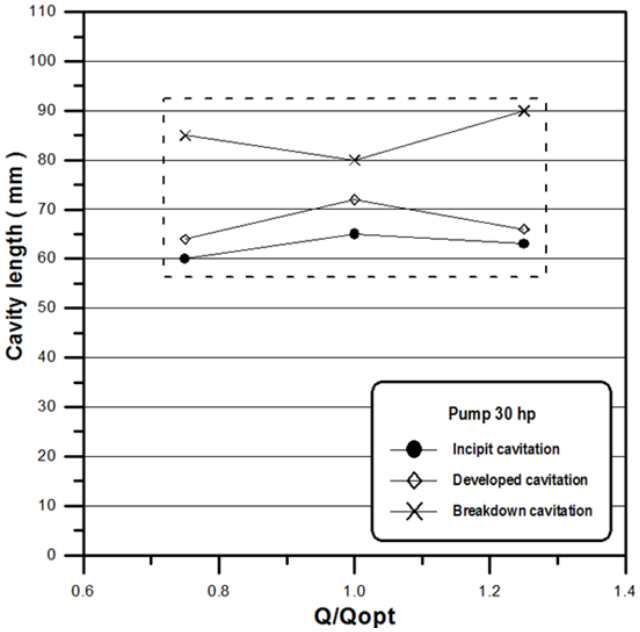

Fig. 18 Variation of cavity length with flow rate ratio for 30 hp centrifugal pump

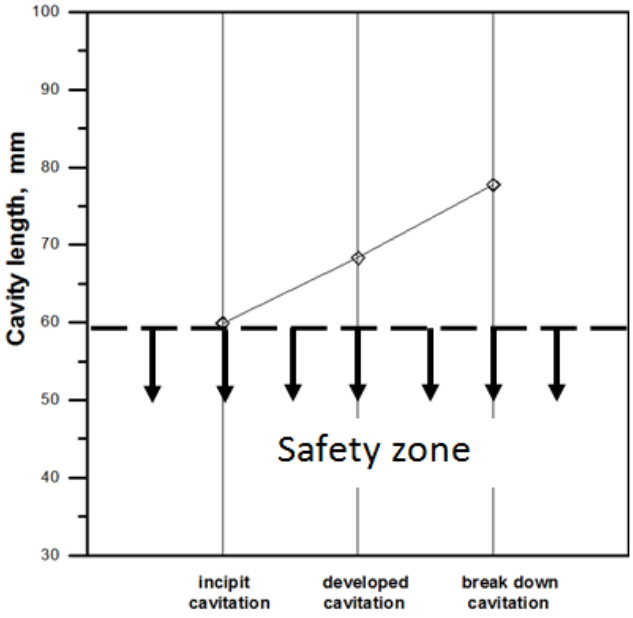

Fig. 19 Average cavity length for all tested pumps

4. Conclusion

1. The cavity length increases gradually from incipit to developed to breakdown cavitation respectively**.**
2. The cavities density increases with the increase of pump power.
3. To avoid any occurrence of cavitation for the tested pumps the cavity length should be less than 60 mm.
4. The whiteness degree of cavities colors increases with the increase of flow velocity and pump power.
5. To operate the pump safe from cavitation the cavity length should exceed 60 mm.

5. References

[1] McNulty PJ, Pearsall IS,"Cavitation inception in pumps". J. Fluids Eng 104(1), 99-104 (Mar 01, 1982)

[2] Hart, D. P. and Brennen, C. E. and Acosta, A. J. "Observations of Cavitation on a Three-Dimensional Oscillating Hydrofoil, (25th : 1990 : Toronto, Ontario). Fluids Engineering Division. Vol.FED-98. No.98. American Society of Mechanical Engineers , New York, pp. 49-52.

[3] Konno, A., Kato, H., Yamaguchi, H. and Maeda, M., "Observation of Cavitation Bubble Collapse by High speed Video", Proceedings of The Fifth Asian Symposium on Visualization, 1999, pp. 134-139.

[4] Kotaro SATO, Masayuki TANADA, Sachie MONDEN, Yoshinobu TSUJIMOTO, " Observations of Oscillating Cavitation on a Flat Plate Hydrofoil", JSME International Journal Series B Fluids and Thermal Engineering, Vol. 45 (2002) No. 3 Special Issue on International Conference on Power and Energy System P 646-654

[5] Sheng-Hsueh Yang Shenq-Yuh Jaw Keh-Chia Yeh,"Single cavitation bubble generation and observation of the bubble collapse flow induced by a pressure wave", Experiments in Fluids, 2009, Vol. 47, pp. 343–355

[6] Ahmed A. B. Al-Arabi1 and Sobeih M. A. Selim, Reality of cavitation inception in centrifugal pumps", 8th Internal Conference on Sustainable Energy Technologies; Aachen, Germany. 31th August – 3rd September, 2009.

[7] Tzanakis, I. and Hadfield, M., "Observations of acoustically generated cavitation bubbles within typical fluids applied to a scroll expander lubrication system", Journal of Hydrodynamics, 2010.

[8] A. A. Alarabi, "Observation and Study of Cavitation in Closed Flow System", 9th International Conference on Heat Transfer, Fluid Mechanics and Thermodynamics 16 – 18 July 2012 Malta.

[9] Bram Verhaagen a, David Fernandez Rivas, "Measuring cavitation and its cleaning effect" Ultrasonics Sonochemistry 29 (2016) 619–628, Elsevier Ltd.

[10] K. Sreedhar, S.K.Albert, A.B.Pandit, "Cavitation damage: Theory and measurements – A review", Wear 372-373 (2017) 177–196, Elsevier Ltd.

[11] Hou-lin Liu, Jian Wang, Yong, Hua Zhang and Haoqin Huang,"The influence of the empirical coefficients of cavitation model on predicting cavitating flow in the centrifugal pimp", Int. J. Nav. Archit. Ocean Eng. (2014) 6:119~131.

[12] Xiongjun Wu⇑, Etienne Maheux, Georges L. Chahine, " An experimental study of sheet to cloud cavitation", Experimental Thermal and Fluid Science 83 (2017) 129–140